Protonation and Conformational Dynamics of GFP Mutants by Two-Photon Excitation Fluorescence Correlation Spectroscopy

C. Bosisio,[†] V. Quercioli,[†] M. Collini,[†] L. D'Alfonso,[†] G. Baldini,[†] S. Bettati,[‡] B. Campanini,[‡] S. Raboni,[‡] and G. Chirico*,[†]

Dipartimento G. Occhialini, Università di Milano Bicocca and Dipartimento di Biochimica e Biologia Molecolare, Università di Parma

Received: February 8, 2008; Revised Manuscript Received: April 30, 2008

GFP mutants are known to display fluorescence flickering, a process that occurs in a wide time range. Because serine 65, threonine 203, glutamate 222, and histidine 148 have been indicated as key residues in determining the GFP fluorescence photodynamics, we have focused here on the role of histidine 148 and glutamate 222 by studying the fluorescence dynamics of GFPmut2 (S65A, V68L, and S72A GFP) and its H148G (Mut2G) and E222Q (Mut2Q) mutants. Two relaxation components are found in the fluorescence autocorrelation functions of GFPmut2: a 10−100 μs pH-dependent component and a 100−500 μs laser-power-dependent component. The comparison of these three mutants shows that the mutation of histidine 148 to glycine induces a 3-fold increase in the protonation rate, thereby indicating that the protonation−deprotonation of the chromophore occurs via a proton exchange with the solution mediated by the histidine 148 residue. The power-dependent but pH-independent relaxation mode, which is not affected by the E222Q and H148G mutations, is due to an excited-state process that is probably related to conformational rearrangements of the chromophore after the photoexcitation, more than to the chromophore excited-state proton transfer.

I. Introduction

A series of proteins from reef animals have been discovered in the past 10 years. Among these, the green fluorescent protein (GFP) from the jellyfish *Aequorea victoria* has been one of the most popular in biology because of its high stability, high production, and quantum yield.[1–3] However, the fluorescence emission of wild-type GFP and mutants displays some degree of flickering. Depending on the mutations within or around the chromophore, the emission wavelength of the protein is shifted, and the excited-state photodynamics undergoes wide variations.[3,4] The study of the internal photodynamics of this class of visible emitting proteins is interesting for at least two reasons. An efficient use of the protein as a cellular marker in microscopy can be made, provided that fluorescence flickering and/or switching is made negligible or very small. The fluorescence fluctuations induce a reduction in the effective quantum yield in bulk measurements, whereas for single-molecule techniques fluorescence flickering limits the use of GFP as a molecular tracer. However, the internal photodynamics can also be used as a sensitive tool within the cell:[5] proton detection,[6–8] redox,[9] and temperature[10] measurements have been reported with specific mutants.

The GFP chromophore, a *p*-hydroxybenzylidene-imidazolidinone tightly held by the beta barrel of the protein, is endowed with a protonation site on the tyrosyl group of residue Y66. Two protonation states of the chromophore,[11,12] neutral (N) and anionic (A), can be detected by spectroscopic methods, and a third zwitterionic (Z) state has been suggested on a theroretical basis.[13,14] The anionic state ($Chro^-$), ascribed to the deprotonated form of the Y66 tyrosyl group,[1] displays absorption and emission at about 475−515 and 505−525 nm, respectively.[3,11,15–18] The neutral state of the chromophore (ChroH), typically dimmer than the anionic one,[3] absorbs at about 375−405 nm and emits both at 440−470 nm and close to the fluorescence of the anionic form. The shorter-wavelength band, usually characterized by low intensity, has been attributed to the direct neutral state de-excitation whereas the green emission, which corresponds to a large Stokes shift, has been ascribed to an excited-state proton transfer (ESPT).[17,18] ESPT is largely affected by the presence of E222 because this residue can act as a proton acceptor of $Chro^-$ through a hydrogen bonding network[16], as suggested by simulations[19] and confirmed recently by time-resolved IR spectroscopy[20] that indicates that the carboxyl group of E222 in wild-type GFP loses a proton within few hundred picoseconds from the neutral chromophore excitation. Additional support for the role of E222 in ESPT comes from the complex picosecond/subnanosecond fluorescence dynamics of GFP mutants[4] and from a reduced ESPT efficiency (>10%) for some E222Q GFP mutants.[3] The emission following the ESPT process occurs from a structurally unrelaxed intermediate state I, with conformational features typical of the neutral state and the protonation state of the anionic form.[1,14,21–24] The ESPT efficiency has been directly measured from bulk absorption and emission spectra of a series of mutants.[3] Apart from wild-type GFP and the T203V mutant, which display an ≅100% ESPT efficiency, none of the mutants investigated by Jung et al.[3] display efficiencies larger than 20%. A number of theoretical works have suggested that the zwitterionic state Z can be considered practically dark[1,4,13,25] and that it is probably due to a proton exchange from E222 to the ammine group of the chromophore. However, no experimental evidence for the zwitterionic nature of some dark states has been reported up to now. GFP flickering might indeed be due, as an alternative to the A−Z transition, to a cis−trans isomerization[25] or to some other protonation state such as those suggested in refs 15 and 40.

* Corresponding author. E-mail: giuseppe.chirico@mib.infn.it. Fax: 39-02-64482447.
[†] Università di Milano Bicocca.
[‡] Università di Parma.

10.1021/jp801164n CCC: $40.75
Published on Web 06/27/2008

Because both the Z and N states are typically much dimmer than the anionic state (except for wild-type GFP and its T203 mutants[3]), the transitions between these states appear as sudden transitions to a dark state in the fluorescence trace. These transitions produce microsecond to millisecond large fluorescence fluctuations when observed on single protein molecules, either immobilized in solid matrices or freely diffusing in solution. With immobilized proteins, the transition rates can be measured directly from the distributions of the on and off times.[26–29] In solution, single molecules diffusing through the observation volume induce fluctuations in the collected fluorescence emission that are due to both diffusion and internal photodynamics and that can be conveniently analyzed by fluorescence correlation spectroscopy (FCS).[13,21,25,30–32] Both experimental approaches measure the fluctuations in the populations of the A, N, and Z states around equilibrium. However, studies on immobilized proteins may be affected by the interaction of the protein with the embedding matrix.[33,34]

Alternative methods to probing the protein internal dynamics, due to either chemical or conformational changes or both, have relied on the induction of a rapid change in the local environment through a variation, for example, of temperature, pressure, or pH. For GFPs, with most of the dynamics being initiated by or somehow related to a change in the protonation state of the chromophore, the most significant experiments can be performed by the pH-jump technique.[35–37] Both the FCS and the pH-jump experiments indicate the presence of multiexponential relaxations in the fluorescence autocorrelation functions (ACFs) or in the fluorescence signal itself. The corresponding processes, with relaxation times that lie in the microsecond to millisecond time range, have been ascribed to protonation and/or conformational dynamics of the GFP chromophore. The excited-state dynamics, such as that determined by ESPT, has been assessed by excited-state lifetime measurements that indicate subnanosecond processes.[3]

Most of the studies on the effect of mutations on GFP spectral and dynamic behavior have focused on two amino acids tightly interacting with the chromophore,[1,3,4] threonine 203 and glutamate 222, and the chromophore itself, specifically the tyrosyl group at position 66. Indeed, the residues that have been reported to affect the GFP fluorescence properties significantly are serine 65, serine 205, threonine 203, histidine 148, and glutamate 222.[1,3,11,16,38–40] The A and N states have been extensively studied by site-directed mutagenesis involving serine 65, threonine 203, and glutamate 222.[3,4] Recent reports have also studied the effects of mutations H148G[35] (pH-jump spectroscopy) and H148E[41] (time-resolved FTIR spectroscopy). Slightly different conformations of the protein (syn−anti transitions of glutamate 222 and threonine 203), coupled to the different protonation states, have been assumed to rationalize the complex phenomenology.

Here we report the analysis of the role of the histidine 148 and glutamate 222 residues on the protonation−deprotonation processes carried out by (FCS) of GFPmut2 (S65A, V68L, and S72A GFP) and its H148G (Mut2G) and E222Q (Mut2Q) mutants. The main aim is to shed some light on the origin of the complex GFP photodynamics that displays pH-dependent and excitation-intensity-dependent components and to try to relate the relaxation rates observed by FCS to the putative protonation−deprotonation processes involving the GFP chromophore and its surrounding hydrogen bonding network.

II. Materials and Methods

Protein. GFPmut2, Mut2G and Mut2Q were expressed and purified as described elsewhere.[35] GFP mutants were dissolved in buffer solutions containing 10 mM citrate and 100 mM phosphate, at the desired pH. The concentration of the buffer was kept constant, because GFP photodynamics has been reported to depend on the buffer concentration.[6]

Optical Setup. The two-photon excitation (TPE) setup was based on a mode-locked Ti:sapphire laser (Tsunami 3960, Spectra Physics, CA) coupled to a Nikon (Japan) TE300 microscope. The laser provides 280 fs pulses on the sample plane[42] at a repetition frequency of 80 MHz in the range of 700−1000 nm. The fluorescence signal, collected by a Plan Apochromat 60× water objective (NA = 1.2, Nikon, Japan), is separated from the excitation beam by a dichroic mirror and further selected by an emission band-pass filter (HQ515/30, emission at 515 nm, full width of 30 nm, Chroma Inc., Brattelboro, VT). The fluorescence signal is split by a nonpolarizing 50% cube splitter and fed directly to two single-photon avalanche diode (SPAD) modules (Perkin-Elmer, Canada; model SPCM-AQR15). The minimum values of the radial and axial fwhm of the microscope point spread function (PSF) are 240 ± 40 and 780 ± 50 nm, respectively, at a wavelength of 800 nm.[42] However, to discriminate between the internal photodynamics and the diffusion contribution to the autocorrelation function (ACF), the excitation volume was changed by reducing the laser beam diameter at the entrance pupil of the objective lens. The excitation volume employed in the following experiments ranges from 0.5 to 1.3 μm^3, corresponding to axial resolutions (fwhm) of ≅0.6−0.76 μm. An estimate of the excitation intensity on the sample is obtained as the average power divided by the area of the PSF in the focal plane (1 mW corresponds to ≅80 kW/cm^2). For one-photon (OPE) confocal FCS measurements, a continuous wave argon laser (2025 Spectra-Physics, Mountain View, CA) tuned to 488 nm was employed. Confocal detection was obtained by inserting a 50 μm pinhole in the detection unit. Fluorescence spectra of samples on the microscope stage were acquired by means of a CCD (DV420A-BV, Andor, IRL)-based spectrometer (MS125, Lot-Oriel, U.K.).

Fluorescence Correlation Functions. The ACFs were acquired in a pseudo-cross-correlation mode in which two replicas of the same signal were detected by two identical detectors. The normalized ACFs were acquired by an ALV5000E (ALV, Langen, D) board and analyzed by means of the nonleast-squares routine of the Origin 7.0 software (OriginLab Inc., Northampton, MA). For all experiments as a function of temperature, the samples were lodged in a homemade Peltier thermostatted cell where the temperature was controlled in the range of (15−65) ± 0.5 °C.

Fluorescence Lifetimes. A PCI board for time-correlated single-photon counting (TCSPC) (Time Harp 200, PicoQuant, Berlin D) was employed to measure the times of arrival (with respect to the laser pulse) of photons collected from protein solutions by the SPAD module. The full half-height width of the intensity response function is ≅350 ps.

III. Results and Discussion

Fluorescence Spectra of GFPmut2. The one-photon absorption spectra of GFPmut2, Mut2G, and Mut2Q indicate two main bands centered at about 395 and 490 nm,[35,19] which, according to the literature,[17,43,44] are ascribed to the neutral and anionic form of the chromophore, respectively. The emission spectra of the three GFP mutants, after excitation of the anionic form at 490 nm, show a large asymmetric band at about 510 nm that is ascribed to the direct de-excitation of the anionic form of the chromophore. When excited at 395 nm, all the three mutants display the same wide

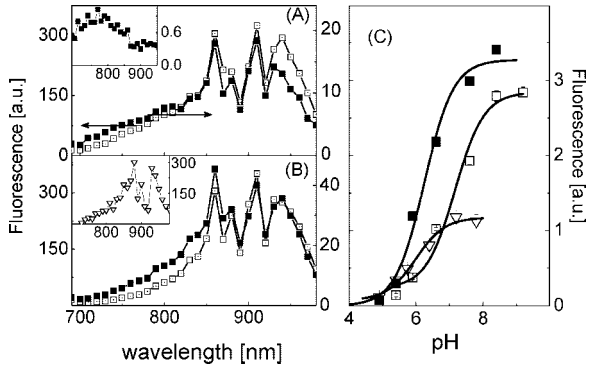

Figure 1. TPE spectra collected on GFPmut2, Mut2G, and Mut2Q. (A) Mut2G excitation spectra collected through the 515/30 band-pass filter (anionic emission) at pH 8.4 (open squares, left axis) and pH 5.9 (filled squares, right axis). The inset reports the excitation spectra collected on the same mutant through the 460/40 band-pass filter (neutral emission) at pH 5.9. (B) GFPmut2 excitation spectra collected through the 515/30 band-pass filter (anionic emission) at pH 8.4 (open squares, left axis) and pH 5.9 (filled squares, right axis). The inset reports the Mut2Q excitation spectrum collected through the 515/30 band-pass filter at pH 8.4. Protein solutions were at a concentration of 2−5 μM, and excitation power was 1.3 MW/cm^2. (C) Plot of the fluorescence at 510 nm as a function of pH. Filled squares, open squares, and open down triangles refer to GFPmut2, Mut2G, and Mut2Q, respectively. The solid lines are the best-fit of eq 1 to the data and correspond to pK = 6.2 ± 0.1, f_0 = −7 ± 17, and Δf = 333 ± 20 for GFPmut2; pK = 7.2 ± 0.2, f_0 = 23 ± 16, and Δf = 260 ± 20 for Mut2G; and pK = 6.0 ± 0.1, f_0 = 7 ± 8, and Δf = 110 ± 8 for Mut2Q.

TABLE 1: Excited-State Lifetime of GFP Mutants[a]

	τ_1 (ns)	τ_2 (ns)	f_1
GFPmut2	3.13 ± 0.04	0.9 ± 0.2	0.92 ± 0.04
Mut2G	3.1 ± 0.1	1.3 ± 0.1	0.87 ± 0.03
Mut2Q	2.13 ± 0.16	0.8 ± 0.1	0.22 ± 0.03

[a] The anionic excited-state lifetime decays in nanoseconds: τ_1 and τ_2 indicate the excited-state lifetime values, and f_1 is the fractional intensity of the longest of the two components. λ_{exc} = 910 nm, λ_{em} = 515 ± 15 nm, and I_{exc} = 11 MW/cm^2. The average is computed over 20−30 measurements on a total of 4 different samples per mutant. The uncertainty indicated is the standard deviation of the data.

asymmetric emission, peaked at 510 nm, with a second very weak component at 440−460 nm (Supporting Information), probably due to an efficient ESPT process to the anionic chromophore state and to direct neutral-state excitation at 395 nm, in agreement with previous literature reports.[3]

The TPE spectra of the three mutants, collected at micromolar protein concentrations, are reported in Figure 1. The spectra collected at $\lambda_{em} \cong$ 515 nm show a broad band centered at about 850−950 nm under both basic and acidic conditions. The Mut2Q mutant shows a marked decrease in the excitation spectrum intensity at 920 nm with respect to the other two mutants (inset in Figure 1B). GFPmut2 and Mut2G display a blue edge shoulder whose amplitude increases when shifting the solution pH to acidic values. This component must therefore be related to the excitation of the neutral state of the chromophore, as confirmed by the excitation spectrum of the neutral form ($\lambda_{em} \cong$ 460 nm), that displays a single broad band in the same wavelength range (Figure 1A, inset). Apart from this blue edge contribution, the major change in the excitation spectrum (λ_{em} = 515 nm) induced by a decrease in the pH consists of a drastic decrease in the overall signal.

The equilibrium between the anionic and the neutral components can be evaluated by following the emission at 510 nm as a function of pH. To compare the results with the FCS data, we have measured the emission spectra on TPE on highly diluted (10−30 nM) samples (Supporting Information). The fitting of the average value of the anionic fluorescence emission versus pH according to the equilibrium

$$F_{510} = f_0 + \frac{\Delta f}{1 + 10^{(pK - pH)}} \quad (1)$$

yields pK values of 6.2 ± 0.1, 7.2 ± 0.2, and 6.0 ± 0.1 for GFPmut2, Mut2G, and Mut2Q, respectively (Figure 1C), in very good agreement with the results obtained in bulk solutions.[35]

Excited State Lifetimes. We have measured the excited-state lifetime (on TPE) of the anionic chromophore state by following the time decay of the fluorescence emission at 515 nm for the three mutants. GFPmut2 and Mut2G show a major (intensity fraction $f_1 \cong$ 90%) component with characteristic time τ_1 = 3.0 ± 0.1 ns (Table 1) whose weight does not change appreciably with pH and a shorter residual component with decay time $\tau_2 \cong$ 0.8−1.2 ns. For the Mut2Q mutant, the intensity fraction of the fast relaxation decay (≅0.8 ns) rises to $f_2 = 1 - f_1 \cong$ 80%, thereby lowering the average lifetime, defined as $\langle\tau\rangle = f_1\tau_1 + (1 - f_1)\tau_2$, to ≅1.1 ns.

Double-exponential decays in GFP emission have been previously reported for a variety of mutants.[3,17,44] The fast component detected here may be due to an additional excited-state relaxation process of the deprotonated chromophore,[3,22] which should involve the glutamate 222 residue, as indicated by the marked increase of the intensity fraction of this fast decay time for Mut2Q.

FCS as a Function of pH at Constant Excitation Intensity. We have collected the ACFs of the fluorescence emission from diluted (≅10 nM) samples of the GFP mutants over a wide range of pH values. Because we are mainly concerned with the internal photodynamics of the GFP chromophore, we have inserted a beam reducer in the excitation optics in order to obtain larger excitation volumes that yield protein diffusion times longer than 1 ms. All experiments were performed in both OPE and TPE modes with similar excitation volumes. The results obtained in the two excitation modes are consistent with each other (for OPE data see Supporting Information), and in the following text we refer to the TPE ACFs only.

Representative ACFs for the three mutants, at different pH values, are reported in Figure 2. In the Figure, the ACFs were normalized in order to have the best superposition in the diffusive time window (lag time <0.8 ms) as shown in the insets. The good agreement of the ACFs above 1 ms ensures that the diffusive motion is not changing appreciably upon pH titration. The diffusive part of the ACFs was fit to a one-component function of type[45]

$$G_D(t) = \frac{\gamma}{\langle N\rangle}\left(1 + \frac{t}{\tau_D}\right)^{-1}\left(1 + \left(\frac{\lambda}{\sqrt{2}\pi\omega_0}\right)^2 \frac{t}{\tau_D}\right)^{-0.5} \quad (2)$$

where N is the average number of molecules in the excitation volume, τ_D is the diffusion time in the focal plane, $\tau_D = \omega_0^2/8D$, D is the translational diffusion coefficient of the protein, and λ is the excitation wavelength. The factor γ in eq 2 is a geometrical factor that accounts for the shape of the excitation volume: when assuming a Gaussian−Lorentzian shape, as in the case of TPE, γ = 0.076,[45,46] whereas for a one-photon confocal setup, $\gamma \cong$ 0.35.[47] By assuming a diffusion coefficient of D_{rh} = 280 μm^2/s for rhodamine 6G at T = 25 °C in water, we measured a typical excitation volume $V_{exc} = \pi\omega_0^4/\lambda \cong$ 1.1 μm^3 (corresponding to $\omega_0 \cong$ 0.7 μm) at λ_{exc} = 910 nm. All of the mutants displayed a diffusion coefficient comparable to that

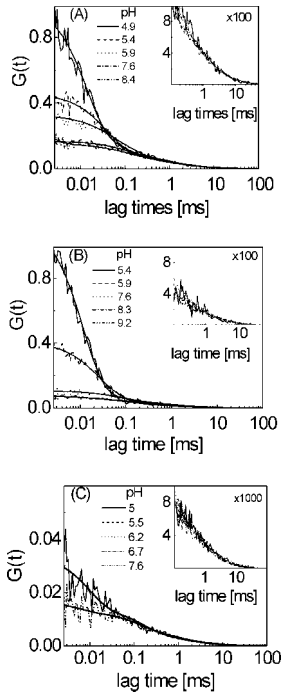

Figure 2. ACFs of diluted (10−30 nM) protein solutions at various pH values, excitation intensity $I_{exc} = 11 \pm 1$ MW/cm^2, $\lambda_{exc} = 910$ nm. Panels A−C refer to GFPmut2, Mut2G, and Mut2Q, respectively. The pH values are indicated in the labels. The insets show, on a log−linear scale, the detail of the diffusive time decay of the ACFs.

of the GFP monomer, $D \cong 90$ μm^2/s, and no systematic dependence on solution pH was detected.

Beside the diffusive relaxation, the ACFs indicate the presence of a composite relaxation decay whose amplitude increases when shifting the pH to acidic conditions, whereas the corresponding relaxation time decreases (Figure 2). To describe the ACF decay over the whole range of lag time acquired, several exponentials should be used according to the model function[30]

$$G(t) = G_D(t) \times \prod_j \left[1 + \frac{A_j}{1 - A_j} \exp(-t/\tau_j)\right] \qquad (3)$$

where A_j and τ_j are the fraction of the jth dark species and the corresponding bright-to-dark transition relaxation time.

All of the ACFs show a triplet contribution ($j = $ T) at very short time delays ($\cong$5 μs), whose amplitude changes with the excitation power up to a maximum of $A_T \cong 0.25$. Because we are not interested in the GFP triplet characterization, triplet-state dynamics has been set aside in the following analysis, and the ACFs have been routinely fitted down to 10 μs, thereby setting $A_T = 0$ for $t < 10$ μs.

To study the role of the chromophore protonation state on the internal photodynamics of GFP mutants, we started by analyzing the ACFs taken at basic pH values: under these conditions (pH >8), few protons are available in solution to protonate the chromophore, and a negligible fraction for the neutral state of the proteins is thereby expected ($A_P = 0$; $j = $ P, "protonation" flickering process). However, a contribution has been found, characterized by a consistent dark fraction for all of the mutants examined. We ascribe this component to a pH-independent relaxation ($j = $ L) with the following amplitudes and relaxation times: $A_L = 0.50 \pm 0.02$ with $\tau_L = 130 \pm 15$ μs for GFPmut2, $A_L = 0.40 \pm 0.04$ with $\tau_L = 160 \pm 20$ μs for Mut2G, and $A_L = 0.40 \pm 0.02$ with $\tau_L = 110 \pm 15$ μs for Mut2Q at $I_{exc} = 11$ MW/cm^2.

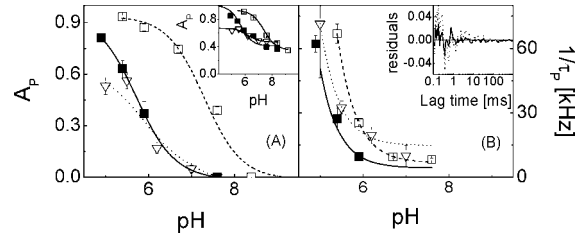

Figure 3. Trend of the fitting parameters of the internal photodynamics versus pH. (A) Fraction of protein molecules in the dark state, A_P, versus pH for GFPmut2 (■), Mut2G (□), and Mut2Q (▽) at $I \cong 11$ MW/cm^2. The relaxation time of the L component was kept at $\tau_L = 130 \pm 15$ μs (GFPmut2), 160 ± 20 μs (Mut2G), and 110 ± 15 μs (Mut2Q). The lines are the best-fit titration curves (eq 1). The best-fit pK values are reported in the text. The inset shows the best-fit dark fraction A_P obtained by fitting the ACFs to eq 3 with $A_L = 0$. (B) Rate, $1/\tau_P$, versus pH (symbols are the same as in panel A). The lines are the best fit of the data to eq 4. (Inset) Residuals of the ACF best fit to eq 3 with single ($A_L = 0$, ---) and double (−) relaxation modes (Mut2G at pH 6.3).

The assumption of pH-independent photodynamics has been made for other GFP mutants.[30] As a matter of fact, by fitting the ACFs to a single-component model over the whole pH range explored ($A_L = 0$ in eq 3) we obtain a dark protein fraction that shows an offset at basic pH values (Figure 3A, inset). We have then chosen to analyze the ACFs versus pH by fixing the pH-independent time decay τ_L to the value found at the corresponding basic pH whereas its fraction (A_L) and the protonation dynamics parameters (fraction A_P and τ_P) are allowed to vary in the fitting procedure. Indeed, the parameter A_L, though left variable in the fitting procedure, does not change appreciably within the pH interval explored. As additional support of the two exponentials model for the GFP photodynamics, we observed that at acidic pH a slight improvement in the fitting residuals is found by using a double-exponential decay (eq 3) for the internal photodynamics, compared with the single-exponential decay ($A_P = 0$ in eq 3; Figure 3B, inset).

The values of the best-fit τ_P and A_P parameters as a function of pH are reported in Figure 3A,B. The trend of the fraction of the pH-dependent relaxation component, A_P, versus pH provides an independent estimate of the deprotonation pK. From the fit of A_P to eq 1 (Figure 3A), we found p$K = 5.8 \pm 0.1$, 7.5 ± 0.1, and 5.9 ± 0.4 for GFPmut2, Mut2G, and Mut2Q, respectively. These values are in good agreement with the results of the analysis of the fluorescence spectra (Figure 1C and Supporting Information) and of bulk measurements reported elsewhere,[35] thereby validating the hypothesis that this component is due to the protonation−deprotonation of the GFP chromophore.

It should be noted that, although for GFPmut2 and Mut2G the dark fraction due to chromophore deprotonation reaches $A_P \cong 90\%$, for Mut2Q only 60% of the molecules reside in the dark state. The different behavior of the three mutants can also be seen directly on the ACFs reported in Figure 2, where a much lower increase in the short time decay at acidic pH is measured for the E222Q mutant ACFs. This finding is apparently not in agreement with only the corresponding bulk experiments (Figure 1C) as a result of minor denaturation effects of low pH values (pH < 5.5), as discussed in the Supporting Information.

The characteristic time of the faster P mode varies from $\cong$10 μs to more than 200 μs when raising the solution pH from 5.5 to 8.5. According to a two-state model, the trend in the relaxation time versus pH can be fit to the equation

TABLE 2: Protonation and Deprotonation Rates and p*K* Values

$k_p \times 10^{-9}$ [M^{-1} s^{-1}]	$k_d \times 10^{-3}$ [s^{-1}]	pK^a	pK^b	pK^c
GFPmut2				
4.6 ± 0.2	4.8 ± 0.8	6.0 ± 0.3	5.8 ± 0.1	6.2 ± 0.1
Mut2G				
15.1 ± 0.3	6.6 ± 0.4	6.4 ± 0.2	7.5 ± 0.1	7.2 ± 0.2
Mut2Q				
5.7 ± 0.5	14.7 ± 1.8	5.6 ± 0.2	5.9 ± 0.3	6 ± 0.1

[a] Values obtained as $pK = -\log(k_d/k_p)$. [b] Values obtained from the fit to eq 1 of the fraction of the dark population, A_P, as a function of pH. [c] Values obtained from the fit to eq 1 of the anionic emission at 510 nm as a function of pH. The values refer to the fit of the TPE autocorrelation functions.

$$\frac{1}{\tau_P} = k_d + k_p 10^{-pH} \tag{4}$$

therefore providing a measure of the protonation, k_p, and deprotonation, k_d, rates. The values of the best-fit parameters reported in Table 2 indicate that the chromophore protonation and deprotonation rates lie in the ranges of 10^9-10^{10} M^{-1} s^{-1} and 10^3-10^4 s^{-1}, respectively. It is noteworthy that the protonation rates of the Mut2G mutant are approximately 3.5 times higher than those of GFPmut2, whereas a 3-fold increase is found in the deprotonation rate of Mut2Q.

A third independent estimate of the p*K* for the photodynamic process comes from the ratio of the deprotonation to the protonation rate constants if we assume that the process is a two-states transition according to

$$pK^* = -\log\left(\frac{k_d}{k_p}\right) \tag{5}$$

As can be seen from Table 2, this estimate of p*K* is also in good agreement with that obtained from the analysis of the emission spectra (Figure 1C) and of the fraction A_P versus the solution pH. An exception is represented by the Mut2G mutant for which we find an ≅16% underestimate that corresponds to an order-of-magnitude under- or overestimate of k_p or k_d, respectively. In the first case, the overestimation of τ_P may be due to the partial superposition of the P and the triplet T decays, and it should amount to ≅30% at most, according to the relation (Supporting Information):

$$\tau_{fit} = \frac{\tau_P}{1 + \frac{f_T}{f_{fit}}\frac{(\tau_P - \tau_T)}{\tau_T}} \tag{6}$$

where $f_T = A_T/(1 - A_T)$ and $f_{fit} = f_T + f_P \cong 1$ and $A_T \cong 0.25$. This effect would correspond to an increase from $pK^* = 6.4$ to ≅6.6 only. However, k_d may be overestimated because of the partial superposition of the L and the diffusive relaxation modes. To account for the observed 16% lower value of pK^* with respect to the bulk estimate, we should have measured $k_d \cong 600$ s^{-1}, a value that is definitely out of the experimental uncertainty of the data (Figure 3B) and of the best-fit parameters.

It is therefore likely that the observed discrepancy between the ACFs and the bulk estimate of the p*K* for Mut2G is not simply due to uncertainties in the experimental data. It must be considered, in fact, that the protonation/deprotonation pathway of the GFP chromophore could be much more complex than the simple two-state model given by eqs 4 and 5, as pointed out by Abbruzzetti et al.[35] The p*K* values obtained should then be regarded as effective values.

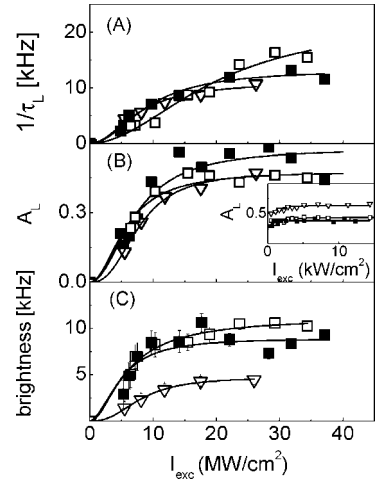

Figure 4. Parameters characterizing the slow relaxation process as obtained from the fit of the ACFs as a function of the excitation intensity I_{exc} at pH 8.5 (λ = 910 nm). (A) Relaxation rate, $1/\tau_L$, versus I_{exc}. Symbols refer to GFPmut2 (■), Mut2G (□), and Mut2Q (▽). The solid lines represent the fit to eq 7. The best-fit parameters are reported and discussed in the text and in Table 3. (B) Fraction of dark molecules, A_L, undergoing fluorescence flickering with characteristic time τ_L versus I_{exc}. The inset of panel B reports the result of a similar analysis on OPE data collected on the three mutants. The best-fit parameters of the solid curves and further details are reported in the Supporting Information. The symbol code is the same as in panel B. (C) Average molecular brightness measured from the ACF and the fluorescence rate as $\langle\varepsilon\rangle = \langle F\rangle G(0)/0.076$ versus I_{exc}.

FCS as a Function of the Excitation Power. The dependence of the best-fit dark fraction A_P on pH (Figure 3) is a clear indication that a protonation process must be involved in this relaxation mode. However, because we are detecting fluorescence, primed either by one- or two-photon absorption, this chemical reaction may occur in either the excited or ground state of the chromophore. Indeed, the excited states typically have stronger polarity; therefore, they are more prone to chemical reactions. To investigate the role of the excited states in the observed photodynamics, we have performed FCS measurements at increasing values of the excitation power at pH ≅5.5 and ≅ 8.5, under TPE. Control measurements upon OPE have been performed as discussed later and in the Supporting Information. We refer explicitly hereafter to TPE data.

At high pH, the ACFs depend remarkably on the excitation power, whereas under acidic conditions no appreciable change is observed in the shape of the ACFs. We have then analyzed the ACFs collected at pH 8.5 at different excitation intensities as described in the previous paragraph by fixing $A_P = 0$: only the pH-independent component is considered because of the high pH value. From the best-fit parameters, we have then obtained the relaxation time τ_L, the dark fraction A_L, the average fluorescence rate F, and the average brightness per molecule $\langle\varepsilon\rangle = \langle F\rangle G(0)/0.076$ (Figure 4). These quantities increase nonlinearly with the excitation intensity, suggesting that the process is limited by photoactivation following two-photon absorption. We have then fit the trend of these parameters with excitation intensity, I_{exc}, with a power law of type[48]

$$\frac{1}{\tau_L} = k_\infty \frac{(I_{exc})^\alpha}{(I_{sat})^\alpha + (I_{exc})^\alpha}$$

$$A_L = A_{L,\infty} \frac{(I_{exc})^\alpha}{(I_{sat})^\alpha + (I_{exc})^\alpha} \tag{7}$$

$$\langle \varepsilon \rangle = \varepsilon_\infty \frac{(I_{exc})^\alpha}{(I_{sat})^\alpha + (I_{exc})^\alpha}$$

where I_{sat} is the laser intensity at which the trend in the spectroscopic parameter as a function of the excitation intensity saturates and k_∞, $A_{L,\infty}$, and ε_∞ are the plateau values at which the corresponding spectroscopic parameters saturate. The exponent α indicates the steepness of the laser excitation intensity dependence of the parameter. These functions describe a multiphoton (for $\alpha > 1$, as found hereafter) activated process that undergoes saturation due to depletion of the ground state or to excitation at higher-energy singlet states.[48] The best-fit parameters obtained from eqs 7 are reported in Table 3.

The trend in the relaxation rate, $1/\tau_L$, corresponds to $\alpha \cong 2$ as expected for a two-photon excited transition (Figure 4A). The vanishing extrapolation of the relaxation rate to $I_{exc} \cong 0$ suggests that the observed process is exclusively photoactivated for all of the studied mutants. The Mut2G mutant reaches a plateau at the highest values of the laser intensity ($\cong$30 MW/cm^2) and reaches the highest value of the limiting rate k_∞. For comparison, the maximum rate for Mut2Q is $k_\infty \cong 10$ MHz, similar to the value measured for GFPmut2, and it saturates at $I_{exc} = 8$ MW/cm^2.

With respect to the relaxation rate $1/\tau_L$, the fraction of dark proteins A_L is characterized by lower saturation intensities, $\cong$6.5 MW/cm^2, for all of the mutants and by a slightly larger value of the exponent, $\alpha \cong 2.9$. It is noteworthy that the limiting value of the dark fraction is very similar for all of the mutants (Figure 4B). This finding does not depend substantially on the excitation mode. In fact, as reported in the inset of Figure 4B, the amplitude A_L measured from the fitting of the ACF collected under the OPE mode ($\lambda_{exc} = 488$ nm, confocal detection) is very similar for GFPmut2 and Mut2G and even slightly larger for Mut2Q (Figure 4B, inset). Further details of the analysis of the OPE data as a function of the excitation intensity are reported in the Supporting Information.

Concerning the molecular brightness (Figure 4C), the best-fit values (Table 3) again indicate a two-photon activated process for all mutants, with $\alpha \cong 2.2 \pm 0.3$ and saturation intensities of $\cong$5 to 6 MW/cm^2, close to those obtained from the fit of the dark fraction. A marked reduction in the molecular brightness of Mut2Q ($\cong$2.5 fold) is observed with respect to the other two mutants. This observation is in agreement with the known effect of mutations at position 222, which largely affect the chromophore fluorescence yield[3] probably as a result of the looser rigidity of the chromophore and its close surroundings. Concerning the origin of the roll-off of the photodynamics trend versus the excitation intensity, we point out that the values of I_{sat} reported in Table 3 are in good agreement with the estimate that can be made of the ground-state S_0 depletion due to the $S_0 \rightarrow S_1$ two-photon induced transition. By assuming a value of the TPE action (cross-section times the quantum yield) of 30 GM (Goeppert−Mayer) for these GFP mutants and an average excited-state lifetime of $\cong$2 ns, we estimate (by imposing a product of the TPE absorption rate times the excited-state lifetime of $\cong$0.5) a value of $I_{sat} = 8$ MW/cm^2, close to the best-fit results reported in Table 3. (For OPE data, see Supporting Information).

TABLE 3: Best-Fit Parameters of the Slower Relaxation Component L as a Function of Excitation Intensity upon TPE ($\lambda_{exc} = 910$ nm)[a]

	k_∞ [MHz]	α	I_{sat} [MW/cm^2]
GFPmut2	13 ± 1.2	2.0 ± 0.6	11 ± 1
Mut2G	22 ± 6	2.0 ± 0.6	20 ± 7
Mut2Q	11 ± 0.6	2.2 ± 0.6	8 ± 0.7
	A_L (∞)	α	I_{sat} [MW/cm^2]
GFPmut2	0.55 ± 0.3	3 ± 1	6.7 ± 0.8
Mut2G	0.48 ± 0.1	3.2 ± 1.8	5.8 ± 0.6
Mut2Q	0.48 ± 0.8	2.6 ± 0.7	7.8 ± 1.4
	ε_∞	α	I_{sat} [MW/cm^2]
GFPmut2	9 ± 0.4	2.5 ± 0.5	4.9 ± 0.5
Mut2G	11 ± 1.2	1.75 ± 0.7	6.2 ± 0.6
Mut2Q	4.7 ± 0.8	2.5 ± 1.5	8 ± 1.8

[a] The best-fit parameters are obtained by fitting eq 7 to the relaxation rate, the dark fraction, and the molecular brightness data. All uncertainties refer to the best-fit variance with the statistical weight of the data.

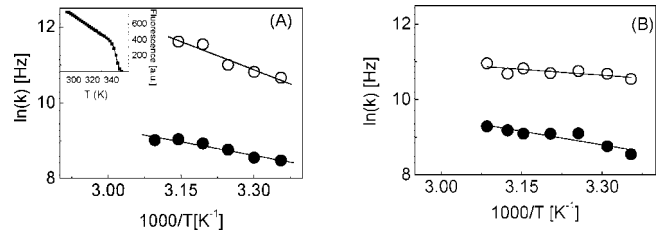

Figure 5. Arrhenius plot of the protonation relaxation rates. (A) GFPmut2. Open symbols refer to the fast P component, and filled symbols refer to the slow L relaxation. (Inset) Average fluorescence signal as a function of temperature ($\lambda_{exc} = 488$ nm, $\lambda_{em} = 505$ nm, and pH= 8.4). (B) Mut2G. Symbols are the same as in panel A.

In conclusion, the excitation intensity dependence of the parameters that characterize the slower relaxation mode is nonlinear, with a square law dependence at low excitation intensity as expected for TPE spectroscopy and a roll off above $\cong$8 MW/cm^2. Indeed, the high correlation between the dark fraction, the relaxation rate and the molecular brightness dependence shown in Figure 4 is a clear indication that the slower relaxation mode is photoactivated by a transition to the same excited state from which fluorescence emission occurs. The slight but significant discrepancy between the trend in the brightness and that of the relaxation rate versus the excitation intensity, observed for Mut2G, suggests a more complex photoactivation pathway, possibly involving higher excited states.

FCS as a Function of Temperature. We have estimated the activation energies of the protonation process by following the change in the relaxation times, τ_P and τ_L, as a function of temperature at pH 5.5 and 8.5, where the fast and slow relaxation processes dominate, respectively. These experiments could be performed for GFPmut2 and Mut2G only: the temperature dependence of the relaxation time could not be measured with sufficient accuracy for Mut2Q because of its low fluorescence yield. A preliminary study of the thermal stability of the GFP mutants has been performed by following the fluorescence signal at increasing temperature (Figure 5, inset). The GFP fluorescence emission is in fact a reliable reporter of the tertiary structure around the chromophore.[49] Apart from a smooth linear decrease in the fluorescence output versus temperature (Figure 5, inset) as a result of the aspecific effects on the chromophore quantum yield, the signal is stable up to $T \cong 65$ °C, and we can therefore assume that below $T \cong 55$ °C the protein retains most of its native structure.

When changing the temperature from 25 to 50 °C at high pH, we observe a decrease in the relaxation time of the L process and a parallel increase in the fraction of dark molecules, A_L. At

low pH values, where two relaxation components are needed to analyze the ACFs, the slow L relaxation component has been set to the value measured at basic pH at the same temperature, whereas the faster P component has been determined by the fitting of the ACFs to eq 3.

The relaxation rates obtained from the inverses of τ_L and τ_P show linear behavior as a function of temperature (Arrhenius plot, Figure 5) from which the corresponding activation energies can be derived. The temperature dependence of the slow "L" relaxation of GFPmut2 and Mut2G corresponds to very similar values of the activation energies, $E_{a,L} = 20.0 \pm 3.0$ and 20.0 ± 3.7 kJ/mol, respectively. For the fast P relaxation, we find instead $E_{a,P} = 42 \pm 5.0$ and 8.4 ± 1.2 kJ/mol for GFPmut2 and Mut2G, respectively.

Because we assumed that the origin of the P relaxation is a protonation−deprotonation process, the values found for the corresponding activation energies should be compared to those reported for proton diffusion in solution, ≅10.4 kJ/mol.[50,51] This value is fairly close to the activation energy found for the Mut2G mutant. For GFPmut2, on the contrary, the corresponding value of the activation energy is much larger, ≅42.0 kJ/mol. This result validates the hypothesis that a swiveling motion of the histidine 148 residue plays a fundamental role in the proton diffusion from the bulk solution to the chromophore, as suggested elsewhere.[35]

The slower relaxation mode is characterized by very similar values of the activation energy for GFPmut2 and Mut2G. The value of about 20 kJ/mol is in good agreement with values found for tiny structural rearrangements in the ground state in GFP.[13]

It is worth noting that two components were also found in the pH-jump-induced relaxation of the optical absorption for the same mutants investigated here.[35] The reported activation energies were very similar, $E_a \cong 29.0 \pm 0.4$ kJ/mol for the two relaxation modes, suggesting that FCS can better discriminate between the different processes and/or mutants.

Origin of the pH-Dependent Relaxation Mode. The faster P relaxation component dominates at low pH, whereas the slower L relaxation is pH-independent. We ascribe the P mode to protonation of the chromophore via proton exchange with the solution, hence the suffix P used for this component. Because this relaxation mode has no marked dependence on the excitation intensity, the corresponding protonation process should take place while the Y66 tyrosyl group is in the ground state.

The proton exchange is likely to occur through histidine 148 that may act either as an entrance gate that binds protons from the solution[35] or as a shutter for the proton far away from GFP.[52] In fact, we find that the protonation rate of Mut2G is at least 3 times faster than that of GFPmut2, whereas the E222Q mutation does not remarkably affect the pH-dependent fluorescence flickering rate. Therefore, histidine 148 seems to be responsible for the transfer of protons from the solution to the chromophore as suggested by refs 19 and 35. This active role of histidine 148 in proton exchange is also supported by the much higher (≅5-fold) activation energy of GFPmut2 compared to that of the mutant where histidine has been replaced by a glycine.

We may then view the external protonation process as a combination of at least two distinct steps. The first is due to proton diffusion in solution that is characterized by low activation energies, in the 10.4 [53]−18.0[52] kJ/mol range, close to the values found for the Mut2G mutant, 8.4 ± 1.2 kJ/mol. The second step might be ascribed to modest conformational changes that involve the histidine 148 residue, and for which we can estimate an activation energy value of ≅34.0 kJ/mol. Indeed, this value is compatible with the activation energies reported for the protonation of surface sites on proteins such as bacteriorhodopsine (≅36 kJ/mol).[54]

Finally, we noticed that the substitution of glutamate 222 with glutamine reduces the protonation probability at acidic pH ($A_P > 0.60$) and increases the deprotonation rate. This is probably due to the stabilizing role played by glutamate 222 in the complex hydrogen bonding network that surrounds tyrosine 66 in its anionic form.[3]

Regarding the comparison of the present data to those previously reported, Abbruzzetti et al.[35] have reported absolute values of the average protonation rate for Mut2G (Table 2 in ref 35) that are approximately 10 times lower than those estimated here (Table 2). This apparent discrepancy may have two possible origins. The fluctuations that occur around the equilibrium condition, detected in FCS experiments, may be intrinsically different from those measured from the decay of the spectroscopic response of the system brought out of equilibrium (pH-jump experiments). Equilibrium and out-of-equilibrium dynamics of a complex system characterized by a rough energy landscape[55,56] can differ substantially, as supported, for example, by the observation of frustrated dynamics in GFP mutants.[57] This possibility may deserve further theoretical and experimental studies that are beyond the scope of the present report.

Alternatively, the different value of the protonation rate measured by FCS and pH-jump experiments may be due to the fact that by these techniques we are probing different steps of the same (i.e., with statistically similar behavior) process. This second issue may also be related to the different excitation mode, OPE or TPE, and to the fact that the change in the fluorescence quantum yield or absorption cross section of the chromophore occurs in only one specific step of the complex kinetic scheme outlined in ref 35 for the chromophore protonation (Table 2 in ref 35). The OPE FCS experiments on the three mutants as a function of the excitation intensity substantially confirm the TPE data analysis (Supporting Information): no dramatic change in the amplitude of the light-induced component is found among the three mutants also under OPE. Therefore, the excitation mode does not seem to be relevant in determining the difference between the FCS and the pH jump experiments (performed under OPE).

The possibility that FCS is probing just one process among the few that characterize the whole protonation−deprotonation kinetics is appealing because of the agreement between the present estimate of the kinetic rate, $\cong 1.5 \times 10^{10}$ [M^{-1} s^{-1}], with that of direct proton exchange

$$\mathrm{ChroH} + \mathrm{His}_{148} \underset{k_{-3}}{\overset{k_3}{\rightleftharpoons}} \mathit{Chro}^- + \mathrm{His}_{148}\mathrm{H}^+$$

between histidine 148 and the chromophore, ChroH, for which Abbruzzetti et al.[35] estimated 10^{10} [M^{-1} s^{-1}] (the k_{-3} parameter in Table 4 of ref 35). This suggests that the fluorescence fluctuations probed by FCS are extremely sensitive to one (the histidine protonation) or a few of the many steps involved in the anionic−neutral transition.(See, for example, Table 4 in ref 35).

Origin of pH-Independent Relaxation Mode. The striking feature of the pH-independent L relaxation found in the ACFs is its low sensitivity to the mutations investigated here. The dependence of the amplitude and the relaxation rate of the L mode on the excitation intensity reflects the excitation mode. In fact, the second power dependence of A_L and $1/\tau_L$ observed at low excitation intensity values under TPE is replaced by a

linear dependence under OPE (Supporting Information). However, the main feature observed under TPE in which the amplitude of the light-driven component, A_L, does not present any dramatic decrease for the two mutants with respect to the parent GFPmut2 protein is substantially confirmed under OPE.

The process involved in this submillisecond flickering is triggered by structural rearrangements of the protein while the chromophore is in its first excited state. Similar relaxation modes, of varying amplitudes, have been reported in the fluorescence ACFs of EGFP and S65T mutants[30] and in a series of mutants involving residues serine 65, glutamate 222, and threonine 203[4] and have been ascribed to an "internal protonation"[30] based on the much lower fluorescence yield of the protonated form of the chromophore. Because ESPT occurs in the excited state and corresponds to charge transfer, the relation between this process and the fluorescence flickering is intriguing, as also discussed in previous FCS studies.[30] In particular, the observed microsecond fluorescence flickering might be due to conformational rearrangements that follow the fast (picosecond) ESPT.

However, because of the putative essential role of glutamate 222 in ESPT, if this process were the origin of the fluorescence flickering, we should observe a dramatic decrease in the dark fraction amplitude, A_L, for the Mut2Q mutant with respect to GFPmut2, which is not the case. For the same reason, the anionic−zwitterionic excited-state conversion, which is assisted by proton donation to the chromophore by glutamate 222, cannot be invoked. Because Mut2G displays similar values of A_L with respect to those of the other two mutants, charge transfer with histidine 148[24,41,58] should not be involved in the light-driven flickering dynamics.

Therefore, it seems likely that the GFP relaxation modes observed by FCS are related to some structural changes in GFP that follow the fast photoinduced isomerization of one of the bonds that build the complex chromophore pocket.[59] Indeed, several possible cis−trans isomerization processes or structural rearrangements in general have been pointed out in the literature: in the chromophore nanoenvironment, threonine 203 and histidine 148 can undergo isomerization,[59] and the chromophore itself has two major relaxation motions related to isomerization around the ϕ angle,[12] or hula-twist motions.[3,13]

As a final remark, we notice that a large number of experiments[19,21,57,60] and most of the considerations drawn in this report indicate a close link between the chromophore and the protein structure. Therefore, it seems appropriate to consider an extended chromophore that also includes a few crucial residues of the protein structure. The finding reported here, that a nonnegligible population of dark protein molecules is present even at basic pH values, should be viewed in this sense. This behavior is similar to that reported by Bizzarri et al.,[19] who assumed the existence of a second group, −XH, beside the tyrosyl group of the chromophore that can convert to the form X^- giving a residual neutral population in the absorption spectra of the E^{n}GFP mutants family.

IV. Conclusions

The GFP photoinduced and ground-state dynamics have been studied for at least 10 years. Few general features have been pointed out, and a comprehensive picture of the behavior of this class of proteins is still being formulated. The reason for these difficulties may lie in the fact that the observed photodynamics pertains to an extended chromophore that undergoes conformational and chemical transitions. The FCS data reported here confirm the important role played by histidine 148 in the proton exchange with the bulk solution. The close agreement between the present estimate of the fluorescence flickering rate and the evaluation of the histidine protonation rate obtained by pH-jump methods[35] suggests that the fluorescence fluctuations in the GFP emission are essentially due to the protonation of histidine 148. The striking result of the present study is that the pH-independent fluorescence fluctuations of the three mutants ascribed to excited-state dynamics are very similar, independent of the excitation mode, OPE or TPE. This finding suggests that little if any role is played by the glutamate 222 or the histidine 148 residues in determining the pH-independent and excitation-dependent photodynamics. These fluctuations should not be directly related to the intramolecular deprotonation of tyrosine 66 but rather to conformational changes of the excited chromophore.

Acknowledgment. This research has been partially funded by project no. 2005-1079 by Fondazione Cariplo to G.C. and PRIN projects 2006 to G.C., G.B., and S.B. We are also grateful to Professor C. Viappiani and Dr. S. Abbruzzetti for useful discussions and to Fondazione Banca del Monte for the donation of the CCD spectrofluorimeter.

Supporting Information Available: Effect of protein denaturation on the autocorrelation functions. One-photon excitation of the neutral state of GFP mutants. Two-photon excitation emission spectra of diluted GFP solutions. Derivation of eq 6. One-photon excitation FCS experiments as a function of the excitation intensity. This material is available free of charge via the Internet at http://pubs.acs.org.

References and Notes

(1) Zimmer, M. *Chem. Rev.* **2002**, *102*, 759.
(2) Lippincott-Schwartz, J.; Patterson, G. H. *Science* **2003**, *300*, 87.
(3) Jung, G.; Wiehler, J.; Zumbusch, A. *Biophys. J.* **2005**, *88*, 1932.
(4) Jung, G.; Zumbusch, A. *Microsc. Res. Technol.* **2006**, *69*, 175.
(5) Kneen, M.; Farinas, J.; Li, Y.; Verkman, A. S. *Biophys. J.* **1998**, *74*, 1591.
(6) Widengren; J.; Rigler, R. *Chem. Phys.* **1999**, 249.
(7) McAnaney, T. B.; Park, E. S.; Hanson, G. T.; Remington, S. J.; Boxer, S. G. *Biochemistry* **2002**, *41*, 15489.
(8) Hanson, G. T.; McAnaney, T. B.; Park, E. S.; Rendell, M. E. P.; Yarbrough, D. K.; Chu, S.; Xi, L.; Boxer, S. G.; Montrose, M. H.; Remington, S. J. *Biochemistry.* **2002**, *41*, 15477.
(9) Bjornberg, O.; Ostergaard, H.; Winther, J. R. *Antioxid. Redox Signal.* **2006**, *8*, 354.
(10) Wong, F. H. C.; Banks, D. S.; Abu-Arish, A.; Fradin, C. *J. Am. Chem. Soc.* **2007**, *129*, 10302.
(11) Brejc, K.; Sixma, T. K.; Kitts, P. A.; Kahn, S. R.; Tsien, R. Y.; Ormo, M.; Remington, S. J. *Proc. Natl. Acad. Sci. U.S.A.* **1997**, *94*, 2306.
(12) Palm, G. J.; Zadnov, A.; Gaitanaris, G. A.; Stauber, R.; Pavlakis, G. N. Wlodawer, A. *Nat. Struct. Biol.* **1997**, *4*, 361.
(13) Weber, W. Helms, V.; Mccammon, J.A.; Langhoff, P. W. *Proc. Natl. Acad. Sci. U.SA.* **1999**, *96*, 6177.
(14) Voityuk, A. A.; Michel-Beyerle, M. E.; Roesch, N. *Chem. Phys.* **1998**, *231*, 13.
(15) Heim, R.; Tsien, R. Y. *Curr. Biol.* **1996**, *6*, 178.
(16) Wachter, R. M.; Elsliger, M. A.; Kallio, K.; Hanson, G. T.; Remington, S. J. *Struct.* **1998**, *6*, 1267.
(17) Chattoraj, M.; King, B. A.; Bublitz, G. A.; Boxer, S. G. *Proc. Natl. Acad. Sci. U.S.A.* **1996**, *93*, 8362.
(18) Lossau, H.; Kummer, A.; Heinecke, R.; Poellinger-Dammer, F.; Kompa, C.; Bieser, G.; Jonsson, T.; Silva, C. M.; Yang, M. M.; Youvan, D. C.; Michel-Beyerle, M. E. *Chem. Phys.* **1996**, *213*, 1.
(19) Bizzarri, R.; Nifosı, R.; Abbruzzetti, S.; Rocchia, W.; Guidi, S.; Arosio, D.; Garau, G.; Campanini, B.; Grandi, E.; Ricci, F.; Viappiani, C.; Beltram, F. *Biochemistry* **2007**, *46*, 5494.
(20) Stoner-Ma, S.; Jaye, A. A.; Ronayne, K. L.; Nappa, J.; Meech, S. R.; Tonge, P. J. *J. Am. Chem. Soc.* **2008**, *130*, 1227.
(21) Liu, Y.; Kim, H-R.; Heikal, A. A. *J. Phys.Chem. B* **2006**, *110*, 24138.
(22) Xie, D.; Zeng, J. *J. Comput. Chem.* **2005**, *26*, 1487.
(23) Voityuk, A. A.; Kummer, A. D.; Michel-Beyerle, M. E.; Roesch, N. *Chem. Phys.* **2001**, *269*, 83.

(24) Leiderman, P.; Huppert, D.; Agmony, N. *Biophys. J.* **2006**, *90*, 1009.
(25) Schwille, P.; S.; Kummer; Heikal, A. A.; Moerner, W. E.; Webb, W. W. *Proc. Natl. Acad. Sci. U.S.A.* **2000**, *97*, 151.
(26) Garcia-Parajo, M. F.; Segers-Nolten, G. M. J.; Veerman, J. A.; Greve, J.; Van Hulst, N. F. *Proc. Natl. Acad. Sci. U.S.A.* **2000**, *97*, 7237.
(27) Peterman, E. J. G.; Brasselet, S.; Moerner, W. E. *J. Phys. Chem. A* **1999**, *103*, 10553.
(28) Jung, G.; Wiehler, J.; Steipe, B.; Brauchle, C.; Zumbusch, A. *ChemPhysChem.* **2001**, *2*, 392.
(29) Baldini, G.; Cannone, F.; Chirico, G. *Science* **2005**, *309*, 1096.
(30) Haupts, U.; Maiti, S.; Schwille, P.; Webb, W. W. *Proc. Natl. Acad. Sci. U.S.A.* **1998**, *95*, 13573.
(31) Hess, S. T.; Heikal, A. A.; Webb, W. W. *J. Phys. Chem. B* **2004**, *108*, 10138.
(32) Cotlet, M.; Goodwin, P. M.; Waldo, G. S. Werner, J. H. *ChemPhysChem* **2006**, *7*, 250.
(33) Moerner, W. E.; Peterman, E. J. G.; Brasselet, S.; Kummer, S.; Dickson, R. M. *Cytometry* **1999**, *36*, 232.
(34) Moerner, W. E. *Proc. Natl. Acad. U.S.A.* **2007**, *104*, 12596.
(35) Abbruzzetti, S.; Grandi, E.; Viappiani, C.; Bologna, S.; Campanini, B.; Raboni, S.; Bettati, S. Mozzarelli, A. *J. Am. Chem. Soc.* **2005**, *127*, 626.
(36) Saxena, A. M.; Udgaonkar, J. B.; Krishnamoorthy, G. *Protein Sci.* **2005**, *14*, 1787.
(37) Mallik, R.; Udgaonkar, J. B.; Krishnamoorthy, G. *Proc. Natl. Acad. Sci. U.S.A.* **2003**, *115*, 307.
(38) Tsien, R. Y. *Annu. Rev. Biochem.* **1998**, *67*, 509.
(39) Cubitt, A. B.; Heim, R.; Adams, S. R.; Boyd, A. E.; Gross, L. A.; Tsien, R. Y. *TIBS* **1995**, *20*, 448.
(40) Labas, Y. A.; Gurskaya, N. G.; Yanushevich, Y. G.; Fradkov, A. F.; Lukyanov, K. A.; Lukyanov, S. A.; Matz, M. V. *Proc. Natl. Acad. Sci. U.S.A.* **2002**, *99*, 4256.
(41) Shu, X.; Kallio, K.; Shi, X.; Abbyad, P.; Kanchanawong, P.; Childs, W.; Boxer, S. G.; Remington, S. J. *Biochemistry* **2007**, *46*, 12005.
(42) Malengo, G.; Milani, R.; Cannone, F.; Krol, S.; Diaspro, A.; Chirico, G. *Rev. Sci. Instrum.* **2004**, *75*, 2746.
(43) Scharnagl, C.; Raupp-Kossmann, R.; Fischer, S. F. *Biophys. J.* **1999**, *77*, 1839.
(44) Creemers, T. M. H.; Lock, A. J.; Subramaniam, V.; Jovin, T. Voelker S. *Nat. Struct. Biol.* **1999**, *6*, 557.
(45) Berland, K. M.; So, P. T. C.; Chen, Y.; Mantulin, W. W.; Gratton, E. *Biophys. J.* **1996**, *71*, 410.
(46) Berland, M.; So, P. T.; Gratton, E. *Biophys. J.* **1995**, *68*, 694.
(47) Bismuto, E.; Gratton, E.; Lamb, D. C. *Biophys. J.* **2001**, *81*, 3510.
(48) Eggeling, C.; Widengren, J.; Rigler, R.; Seidel, C. A. M. *Anal. Chem.* **1998**, *70*, 2651.
(49) Campanini, B. Bologna, S.; Cannone, F.; Chirico, G.; Mozzarelli, A.; Bettati, S. *Protein Sci.* **2005**, *14*, 1125.
(50) Mezer, A.; Friedman, R.; Noivirt, O.; Nachliel, E.; Gutman, M. *J. Phys. Chem. B* **2005**, *109*, 11379.
(51) Luz, Z.; Meiboom, S. *J. Am. Chem. Soc.* **1964**, *86*, 4768.
(52) Yoshino, A.; Yoshido, T.; Takahashi, K. *Magn. Reson. Chem.* **1989**, *27*, 344.
(53) Agmon, N. *Isr. J. Chem.* **1999**, *39*, 493.
(54) Heberle, J.; Dencher, N. A. *Proc. Natl. Acad. Sci. U.S.A.* **1992**, *89*, 5996.
(55) Frauenfelder, H.; Leeson, D. T. *Nat. Struct. Biol.* **1998**, *5*, 757.
(56) Frauenfelder, H. *J. Biol. Phys.* **2005**, *31*, 413.
(57) Andrews, B. T.; Schoenfish, A. R.; Roy, M.; Waldo, G.; Jennings, P. A. *J. Mol. Biol.* **2007**, *373*, 476.
(58) Agmon, N. *Biophys. J.* **2005**, *88*, 2452.
(59) Agmon, N. *J. Phys. Chem. B* **2007**, *111*, 7870.
(60) Baldini, G.; Cannone, F.; Chirico, G.; Collini, M.; Campanini, B.; Bettati, S.; Mozzarelli, A. *Biophys. J.* **2007**, *92*, 1724.

JP801164N